Development of a new chitosan/Ni(OH)(2)-based sorbent for boron removal

H. Demey, Thierry Vincent, M. Ruiz, A. M. Sastre, E. Guibal

Development of a new chitosan/$Ni(OH)_2$-based sorbent for boron removal

H. Demey [a,b,*], T. Vincent [b], M. Ruiz [a], A.M. Sastre [c], E. Guibal [b]

[a] Universitat Politècnica de Catalunya, Department of Chemical Engineering, EPSEVG, Av. Víctor Balaguer, s/n, 08800 Vilanova i la Geltrú, Spain [b] Ecole des mines d'Alès, Centre des Matériaux des Mines d'Alès, 6 Avenue de Clavières, F-30319 Alès Cedex, France
[c] Universitat Politècnica de Catalunya, Department of Chemical Engineering, ETSEIB, Diagonal 647, 08028 Barcelona, Spain

ABSTRACT

A new composite containing chitosan (as the encapsulating material) and nickel (II) hydroxide [chiNi(II)] has been manufactured for the removal of boron from aqueous solutions. The biosorbent was character-ised using SEM and TGA analyses. Sorption uptake was highly dependent on pH, temperature, initial boron concentration and the mass of the adsorbent. The optimum pH for boron removal was approxi-mately 8. The sorption isotherms were fitted with the Langmuir and the Freundlich models. The Langmuir equation gave the best fit of the experimental data; the maximum adsorption capacity was 61.4 mg g^{-1}. The uptake kinetics was modelled using the pseudo-second order rate equation. Metal elution was per-formed using an aqueous solution with the pH set to 12 with NaOH. The recycling of the sorbent was tested, maintaining a removal efficiency and a metal recovery over 90% for five successive sorption/desorption cycles. The effect of temperature was also evaluated, verifying the exothermic nature of the adsorption process.

HIGHLIGHTS

- A new composite containing chitosan and nickel (II) hydroxide has been manufactured.
- [chiNi(II)] composite was used as adsorbent for boron removal.
- Adsorption–desorption cycles were performed and desorption uptake remained >90%.
- High NaCl concentration does not affect boron removal.
- The temperature study confirmed the exothermic nature of boron sorption.

GRAPHICAL ABSTRACT

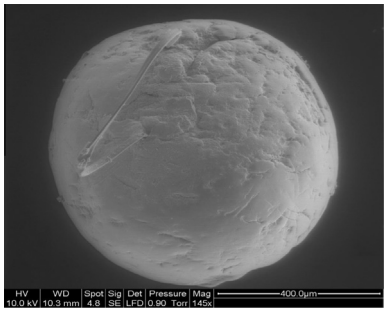

Keywords:
Boron
Chitosan
Nickel
Composite
Sorption
New sorbent

1. Introduction

The boron present in the environment occurs either naturally or as a result of human activity (mainly in the form of boric acid or borate salts). Water contamination by boron is one of the most widespread environmental problems because boron compounds are widely used in the manufacture of heat resistant glass, soaps, detergents, pesticides, cosmetics, fertilisers in agriculture, etc. Ostürk et al. [1] regards boron as one of the most important micro-nutrients for plants. Although it is essential for plant life and small amounts of boron can even be beneficial for humans, high levels can prove toxic. Indeed, the ingestion of large amounts of boron

* Corresponding author at: Universitat Politècnica de Catalunya, Department of Chemical Engineering, EPSEVG, Av. Víctor Balaguer, s/n, 08800 Vilanova i la Geltrú, Spain. Tel.: +34 938937778; fax: +34 934017700.
E-mail address: hary.demey@upc.edu (H. Demey).

affects the central nervous system and the reproductive system of human beings [1]. The World Health Organization has stated that short- and long-term oral exposures to boric acid or borax in laboratory animals have shown the male reproductive system to be a consistent target of toxicity. Testicular lesions have been observed in rats, mice and dogs given boric acid or borax in food or drinking water. The guide level for boron in drinking water was set to 2.4 mg L^{-1} [2]. For environmental protection, an efficient solution must be provided to remove boron compounds from water and to reduce the boron concentration below the permissible level before being discharged into the environment. In addition, boron is a major concern for the desalination of sea water [3].

Several different methodologies have been applied for boron removal, such as adsorption with clays [4] and fly ash [5], ion exchange with boron-specific resins [6,7], reverse osmosis [8–10], electrodialysis [11], precipitation [12], chemical coagulation and electrocoagulation [13,14].

It is commonly known that sorption is the most competitive process for boron removal/recovery, and for the last decade, great attention has been paid to development of new low-cost sorbents. Low operating costs and the availability of the necessary resources are the main criteria for the selection of alternative sorbents. These adsorbents can be reusable waste materials from industries or even natural materials; e.g., Demey et al. [15] and Ruiz et al. [16,17] have used calcium alginate beads to effectively separate boron from aqueous solutions.

Some authors have shown the potential of biopolymers for the immobilisation of active materials and the elaboration of composite adsorbents. Gazi and Shahmohammadi [18] removed traces of boron from aqueous solutions using chitosan beads modified by grafting imino-bis-(propylene glycol) moieties onto the beads. Wei et al. [19] designed an environmentally friendly adsorbent for boron removal by functionalisation of chitosan by the N-methylglucamine group through atom transfer radical polymerisation. However, these materials require a delicate and meticulous manufacturing process, and Wei et al. [19] did not report the boron desorption from these materials. A good sorbent, especially for large-scale applications, need to be recyclable to be competitive. Maximum boron adsorption with chitosan beads was reported as 0.3 mg g^{-1}; hydroxyl and amino groups of chitosan play an important role in the removal of boron from aqueous solutions [19].

Adsorption/co-precipitation of boron from aqueous solutions was investigated by Turek et al. [20] using the metal hydroxides $Ni(OH)_2$, $Zn(OH)_2$, $Co(OH)_2$, $Mg(OH)_2$, $Fe(OH)_3$ and $Al(OH)_3$, and it was found that nickel hydroxide was the most effective of the hydroxides studied. The relative reactivities follow this order: Ni(II) > Al(III) > Co(II) > Fe(III) > Zn(II) ≈ Mg(II). The present study addresses the development of a new composite [chiNi(II)], made of chitosan and nickel (II) hydroxide, for the recovery of boron from aqueous solutions. Chitosan–Ni solution in contact (dropwise) with NaOH solution coagulates easily; thus, the formation of nickel (II) hydroxide in situ as regular beads using chitosan is a low-cost and efficient encapsulation technique. With this composite, the best operating conditions were implemented for boron recovery that avoided Ni(II) release into the solution. Environmental parameters affecting the adsorption process such as temperature, pH and the initial boron concentration were studied. The equilibrium adsorption data were evaluated using the Langmuir and the Freundlich isotherms models. The uptake kinetics for boron removal has also been investigated, and the pseudo-first order and pseudo-second order models were evaluated to fit the experimental data: two different ways to dry the sorbents (air-drying and freeze-drying) were compared for their effect on the kinetics profiles.

2. Experimental

2.1. Materials

Boron solutions were prepared using boric acid ($B(OH)_3$) provided by Merck AG (Germany). Nickel (II) nitrate hexahydrate was used for sorbent preparation and was provided by Panreac (France).

Chitosan was supplied by Aber Technologies (France), and its molecular weight (125,000 g mol^{-1}) was previously reported by Ruiz et al. [21] using size exclusion chromatography (SEC) coupled with light scattering and refractometry. The degree of deacetylation determined by Fourier Transform infrared (FTIR) spectroscopy was found to be 87% [22].

2.2. Preparation of [chiNi(II)] composite microspheres

The chitosan solution, with a concentration of 1% w/w, was prepared by dissolving 1 g of chitosan in 1% w/w acetic acid solution and stirring for at least 3 h. Forty grams of $Ni(NO_3)_2.6H_2O$ powder were mixed in 120 mL of HCl solution (1 M) until complete dissolution. The chitosan solution (640 g, 1% w/w) was then mixed with nickel (II) solution under vigorous stirring (600 rpm) for 120 min.

The chitosan-nickel (II) solution was added drop-by-drop with a peristaltic pump through a thin nozzle (Ø 1.6 mm) into an aqueous solution of 1 M sodium hydroxide under magnetic stirring to produce microspheres of the composite chitosan/nickel (II) hydroxide [chiNi(II)].

The composite particles were kept under stirring for 6 h at room temperature (25 °C), and then were filtered and intensively washed with distilled water to remove the excess of nickel present on the surface of the composite beads. Subsequently, the beads were washed with ethanol and then were kept at room temperature (25 °C) for 48 h to dry. The average diameter of air-dried beads (the reference material used in this work) was 0.85 mm.

To verify the stability of the sorbents, three different nickel concentrations were used in the preparation of the air-dried beads, following the same procedure:

- B40 (reference material used in this work): 40 g of $Ni(NO_3)_2{\cdot}6H_2O$, 120 mL of 1 M HCl and 640 g of chitosan 1% w/w.
- B10: 10 g $Ni(NO_3)_2{\cdot}6H_2O$, 30 mL of 1 M HCl and 640 g of chitosan 1% w/w.
- B5: 5 g of $Ni(NO_3)_2{\cdot}6H_2O$, 15 mL 1 M HCl and 640 g of chitosan 1% w/w.

The mass percentage of $Ni(OH)_2$ in B40, B10 and B5 composites was determined using chemical mineralization by reaction with a 18 M sulfuric acid solution at boiling temperature followed by successive additions of 1 mL of hydrogen peroxide (30% w/w) until complete discoloration [23]. The nickel solutions were analyzed with an inductively coupled plasma atomic emission spectrometer ICP-AES (HORIBA JOBIN YVON, FRANCE) at a wavelength of 221.6 nm. The mass percentages were 72%, 45% and 18% of $Ni(OH)_2$ per gram of composite in B40, B10 and B5, respectively. B40 (air-dried beads) is the reference material used in most of the experiments in this study.

To compare the effect of the drying method on the kinetic profiles, wet samples of [chiNi(II)] (without a prior ethanol wash) were freeze dried using a freeze dryer (Bioblock scientific, Christ) at 223 K and 0.01 mbar.

2.3. Characterisation of the sorbents

2.3.1. Scanning electron microscopy

The samples were analysed using the environmental scanning electron microscope (ESEM) Quanta FEG 200, a type of high-performance scanning electron microscope (SEM) specialised for use in low-vacuum, high vacuum and the so-called environmental SEM mode. This makes possible the analysis of samples under pressures up to 6.6×10^{-3} bar. Additionally, the microscope is equipped with a Schottky field emission gun (FEG) for optimal spatial resolution and with an Oxford Inca Energy Dispersive X-ray (EDX) system for chemical analysis.

The samples of adsorbents were analysed before and after boron adsorption. Though the boron signal was too low to be measured, SEM–EDX analysis was used to detect the main elements present at the surface of the sorbent particles.

2.3.2. Thermogravimetric analyses

Thermogravimetric analyses were performed under a nitrogen flow of 20 mL min^{-1} at a heating rate of 10 °C min^{-1}, within a temperature range of 30–800 °C, using a Perkin–Elmer TGA 6 instrument. Sample weights of approximately 20 mg were used in these experiments.

2.3.3. FTIR analysis

Fourier transform infrared (FTIR) analysis of the sorbents was performed on a BRUKER IFS 66 FTIR spectrophotometer equipped with a reflection diamond accessory (platinum ATR), and the spectra were recorded in the range of 4000–400 cm^{-1}. Two samples of 2 mg of [chiNi(II)] (before and after boron adsorption) were used for FTIR analysis.

2.4. pH effect

The study of pH-influence on boron removal was performed by mixing 100 mL of boron solution (50 mg L^{-1}) with known amounts of adsorbent (0.1 g) in 250-mL polyethylene flasks. Proton concentration was adjusted using 0.1 M HCl and 0.1 M NaOH (initial pH range 3–11), and the stirring speed was set at 100 rpm at 20 °C, using an agitator Rotabit, J.P. Selecta (Spain). After 72 h of agitation, the final pH was measured, and 5 mL of solution were filtered and analysed with an inductively coupled plasma atomic emission spectrometer ICP-AES (HORIBA JOBIN YVON, France) at the wavelength of 249.7 nm for boron and 221.6 nm for nickel.

2.5. Equilibrium sorption

Mono-component sorption isotherms were obtained by mixing a known volume of solution at different boron concentrations at a pH of 3.5, 7 or 11 and a fixed mass of adsorbent (0.1 g) in 100 mL of boron solution. After 72 h of contact, the pH of the solution was measured and the residual concentration of boron (and eventually nickel) was analysed.

The Langmuir and Freundlich models were used to describe the experimental adsorption isotherm data. The Langmuir and Freundlich isotherms are represented by the following equations, respectively [24,25]:

$$q = \frac{q_{max} b C_{eq}}{1 + bC_{eq}} \tag{1}$$

$$q = K_F C_{eq}^{1/n} \tag{2}$$

where q is the amount of boron adsorbed per gram of sorbent at equilibrium (mg g^{-1}), q_{max} is the maximum adsorption capacity of the adsorbent (mg g^{-1}), and C_{eq} is the equilibrium concentration of the solution (mg L^{-1}). In the Langmuir model (Eq. (1)), b is related to the energy of adsorption (L mg^{-1}), whereas K_F and n are the Freundlich adsorption constants, indicative of the relative capacity and the adsorption intensity, respectively.

2.6. Influence of contact time

The uptake kinetics experiment was performed by adding (under continuous stirring) a known amount of adsorbent (i.e., 2.5 g) to 500 mL of boron solution (50 mg L^{-1} and 5 mg L^{-1}) at pH 11. Aliquots of adsorbate were withdrawn at different times and filtered after 120 h of contact. The residual concentration was determined by ICP-AES. The kinetic profiles were compared for three different conditions of the beads:

- Air-dried beads (Ø 0.85 mm).
- Freeze-dried beads (Ø 2.0 mm).
- Wet beads (Ø 2.0 mm).

The intraparticle diffusion equation [26] and the pseudo-first and pseudo-second order model were applied to fit the experimental data. These models are frequently used to describe the batch sorption system:

Pseudo-first order rate equation (PFORE) [27]:

$$\frac{dq_t}{dt} = K_1(q_1 - q_t) \tag{3}$$

Integrating for the boundary conditions $t = 0$ to $t = t$ and $q_t = 0$ to $q_t = q_t$:

$$\log(q_{eq} - q_t) = \log(q_{eq}) - \frac{K_1}{2.303} t \tag{4}$$

Pseudo-second order rate equation (PSORE) [28]:

$$\frac{dq_t}{(q_{eq} - q_t)^2} = K_2 d_t \tag{5}$$

Integrating for the boundary conditions $t = 0$ to $t = t$ and $q_t = 0$ to $q_t = q_t$:

$$\frac{1}{q_t} = \frac{1}{K_2 q_{eq}^2} + \frac{1}{q_{eq}} t \tag{6}$$

where q_{eq} is the equilibrium sorption capacity (mg g^{-1}), q_t is the sorption capacity (mg g^{-1}) at any time t (min) and k_2 is the pseudo-second order rate constant (g mg^{-1} min^{-1}).The parameters q_{eq} and k_2 are pseudo-constants depending on the experimental conditions.

The intraparticle diffusion equation is [26]:

$$q_t = K_p t^{1/2} + C \tag{7}$$

where C is the intercept, and K_p is the intraparticle diffusion rate constant.

Crank's equation was used to determine the intraparticle diffusion coefficient D_e (effective diffusivity, $cm^2\ s^{-1}$), assuming the solid to be initially free of metal [29].

$$\frac{q_t}{q_{eq}} = 1 - \sum_{n=1}^{\infty} \frac{6\alpha(\alpha+1)\exp\left(\frac{-D_e q_t^2 t}{r^2}\right)}{9 + 9\alpha + q_n^2\alpha^2} \tag{8}$$

$$\tan q_n = \frac{3q_n}{3 + \alpha q_n^2} \tag{9}$$

$$\frac{q_{eq}}{VC_o} = \frac{1}{1+\alpha} \tag{10}$$

2.7. Effect of temperature

The temperature influence was evaluated in batch systems using four temperatures (20, 35, 50 and 60 °C), and a known volume of boron solution (0.1 L) at different initial concentrations (1, 5, 10, 15, 25, 40 and 50 mg L^{-1}). Thermodynamic parameters such as the Gibbs free energy change ($\Delta G°$), the standard entropy change ($\Delta S°$) and the standard enthalpy change ($\Delta H°$) were established using the following equations:

$$\Delta G^{\circ} = -RT\ln Kc \tag{11}$$

$$Kc = \frac{C_s}{C_{eq}} \tag{12}$$

$$\ln Kc = -\frac{\Delta H^{\circ}}{RT} + \frac{\Delta S^{\circ}}{R} \tag{13}$$

The standard entropy change ($\Delta S°$) and the standard enthalpy change ($\Delta H°$) were yielded from the van't Hoff equation as shown in Eq. (13), plotting $\ln Kc$ vs $1/T$, where Kc is the equilibrium constant and R is the gas constant 8.314×10^{-3} kJ mol^{-1} K^{-1}.

2.8. Adsorption–desorption experiments

Several adsorption–desorption cycles were performed using 100 mL of a 0.01 M NaOH solution as the desorbing agent, to evaluate the possibility to recycle [chiNi(II)]. Different initial boron concentrations were employed (1, 5, 10, 15, 25, 40 and 50 mg L^{-1}) and the amount of adsorbent used was 2.5 g. After each cycle, composites were washed with distilled water and their efficiency for the adsorption of boron in repeated cycles was monitored and compared. The efficiency of the adsorption and the desorption of boron was determined by the following equations:

$$\%\ \text{Adsorption} = \frac{C_o - C_{eq}}{C_o} \cdot 100 \tag{14}$$

$$\%\ \text{Desorption} = \frac{C_{ed}}{C_o - C_{eq}} \cdot 100 \tag{15}$$

where C_0 is the initial boron concentration (mg L^{-1}), C_{eq} is the equilibrium concentration (mg L^{-1}) during the sorption step, and C_{ed} is the equilibrium boron concentration in the eluent (mg L^{-1}).

3. Results and discussion

3.1. Characterisation of sorbents

3.1.1. Scanning electron microscopy

Fig. 1 shows the sphericity of the sorbent material (Fig. 1a): the particles have an average diameter of 0.85 mm. Small cavities can be observed over the entire surface of the material (Fig. 1b). Fig. 1c shows the cross-sectional surface of a freeze-dried adsorbent. The EDX-analysis in different zones of the cross-section of the adsorbent (Fig. 1c and d) suggest that the elements are homogeneously distributed in [chiNi(II)] materials. Indeed, Ni(II) element (tracers of the active component; i.e., $Ni(OH)_2$) and the elements C and O (tracers of the encapsulation material; i.e., chitosan) were detected at the same magnitude in the different zones of the cross-sectional area.

3.1.2. Thermogravimetric analysis

Thermogravimetric analysis (TGA) measures the amount and the rate of the change in the weight of a material as a function of temperature or time under a controlled atmosphere. Measurements are used primarily to predict a material's thermal stability over a range of temperatures. The technique can characterise materials that exhibit weight loss or gain due to decomposition, oxidation or dehydration.

The composite material [chiNi(II)] has a significant weight loss at approximately 260 °C (see Fig. AM1, in the Additional Material Section). At temperatures below the onset point (258.5 °C, 92.3%) the adsorbent is thermally stable despite a slight weight loss initially observed in the plot that is due to the presence of residual water in the samples. The first derivative was calculated for a better comprehension of the data and to determine the temperature at which the greatest weight loss of the adsorbent occurs. The inflection point indicates a temperature of 430.5 °C, and the remaining weight percentage reached 43%, corresponding to the nickel used for manufacturing the composite sorbent.

3.1.3. FTIR analysis

FTIR spectra were compared for [chiNi(II)] before and after boron sorption (see Fig. AM2, in the Additional Material section). To clarify the differences, the spectrum of the raw sorbent was subtracted from the spectrum of the boron-loaded sorbent.

The strong band centered at 3600 cm^{-1} in [chiNi(II)] spectra is attributed to the presence of non-hydrogen-bonded –OH groups, which provide the characteristic feature of ß-nickel hydroxide present in the composite, as well as the –OH groups of chitosan [30]. The peak at 2922 cm^{-1} is associated with the –CH– stretching vibration of chitosan [18]. The study of metal adsorption onto chitosan showed that in the case of Ni(II), the loaded chitosan presented a characteristic shift compared with non-loaded with Ni(II) in the range of 1672–1638 cm^{-1}, suggesting a metal-chelated complex [31]; this shift is observed in the spectrum of Fig. AM2. N–H bending vibration appeared at 1498 cm^{-1} and deformation vibration at 1395 cm^{-1}, consistent with Bursali et al. [32]. The band at 1025 cm^{-1} in the [chiNi(II)] spectra represents the C–O stretching mode of chitosan [18], and the band centered at 600 cm^{-1} is attributed to an in-plane Ni–O–H bending vibration [33].

Subtraction of the raw sorbent spectrum from the spectrum of the boron-loaded sorbent allowed observation of boron interactions with the composite. A broad band observed at 3370 cm^{-1} corresponds to B–OH stretching vibrations [32]. Broad B–O stretches of the trigonal borate appear in the region of 1300–1480 cm^{-1} [34]; the peak at the 1348 cm^{-1} band can be attributed to B–O stretching, and the peak at 1455 cm^{-1} represents the stretching vibration. An important factor in boron adsorption is the appearance of the band at 1204 cm^{-1}, typical of the C–O bonds that form part of esters.

3.2. pH effect

The pH is an important parameter for the optimisation of the sorption process because the possible interference of protons with the sorbate and/or the sorbent may affect the efficiency of the material [35]. Fig. 2a shows the influence of pH (in the range of 3–12) on boron removal using [chiNi(II)].

The best results were obtained in the range of pH 3–9; above a pH of 9 the sorption efficiency tended to decrease. In addition, Fig. 2b shows the pH variation during boron sorption: the equilibrium pH stabilised around pH 8 when the initial pH was below 9, while above pH 9 the equilibrium pH was hardly changed. It can be attributed to the acid-basic properties of chitosan; chitosan in acidic media is a cationic polymer; according to Sorlier et al. [36], the pKa of chitosan depends on parameters such as the deacetylation degree and the ionisation extent of the polymer. The pKa for standard samples varies between 6.3 and 6.8; chitosan tends to bind protons (amine protonation) when the pH is below pKa, which increases the pH. This type of 'buffering effect' can also

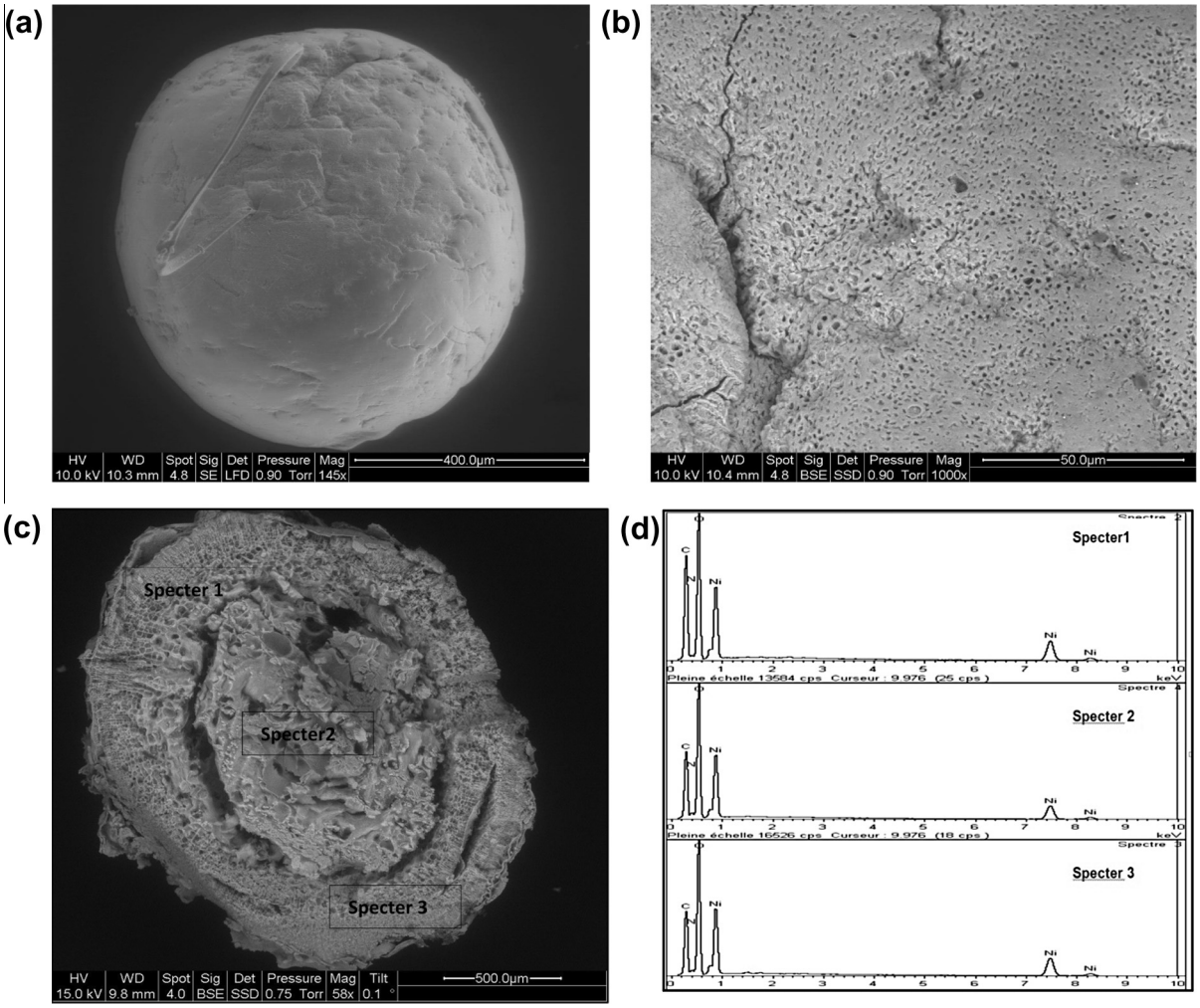

Fig. 1. SEM Images. (a) Topography of the [chiNi(II)] composites. (b) Surface of the [chiNi(II)] composites. (c) Cross section of the freeze dried adsorbent. (d) EDX-analysis of the cross-section of the adsorbent (after boron removal).

explain that boron removal was almost constant in acidic media (Fig. 2a).

Below pH 6.5 the dissociation of nickel (II) hydroxide in the composite material may cause the release of OH^- ions and a relative increase in the pH. This also means that in acidic solutions, Ni(II) ions may be released into the solution, causing environmental impacts. For these different reasons, it appears that the optimum pH will be close to a pH of 8 for reaching a high efficiency, a stable pH and sorbent stability. Further experiments have been performed at this optimum pH value.

Previous experiments have demonstrated that only chitosan cannot remove significant amounts of boron from aqueous solutions: Wei et al. [19] have reported a sorption capacity as low as 0.39 mmol g^{-1} using crosslinked chitosan beads (CCTS).

Boron and nickel speciation depend on the pH and the concentration. In the case of boron, the relative concentration of the $B(OH)_4^-$ anion increases with increasing pH until it becomes the dominant species at a pH of approximately 9.2 (Fig. AM3). In dilute solutions, boric acid is monomeric, but at a concentration above 0.1 M, polymeric species become significant. Formation of these species is a direct result of the tendency of boron to form complexes with electron-donor species including, oxygen (present on borate anions). Eq. (16) reports the dissociation reaction of boric acid (monomeric form) ($K_a = 5.80 \times 10^{-10}$ mol L^{-1}). According to Pagznl et al. [37], in neutral dilute solutions, boric acid represents more than 99% of total boron. Boric acid is a Lewis acid and can bind a hydroxyl ion, forming the borate anion. Both boric acid and borate can react with a suitable dihydroxy compound, resulting in the boric acid ester and the borate monoester, respectively [38].

$$B(HO)_3 + H_2O \leftrightarrow B(OH)_4^- + H^+ \quad (16)$$

Nickel (II) ions may be hydrolysed in solution according Eq. (21). The constant for Ni(II) hydrolysis is $\beta = 1.15 \times 10^{-17}$ [39]. Fig. AM3 displays the speciation diagram for Ni(II) (at a concentration of 100 mmol L^{-1}). For pH < 6.5, the ion Ni(II) is the most abundant species, at a pH of 6.5 the solution contains an equimolar concentration of Ni(II) and $Ni(OH)_2$, and for pH $\geqslant$ 6.5, $Ni(OH)_2$ becomes the predominant species. Nickel (II) hydroxide precipitation begins at pH = 5.5–6, and the solubility product is 1.6×10^{-14} [33].

$$Ni^{+2} + 2H_2O \leftrightarrow Ni(OH)_2 + 2H^+ \quad (17)$$

Furthermore, two possible interactions (Eqs. (18) and (19)) are proposed when the nickel composites are in contact with boron solutions. These mechanisms may only take place if the distances among adjacent OH^- groups in the $Ni(OH)_2$ structure are similar (or of the same order of magnitude) to those observed for boric acid (and borate ions).

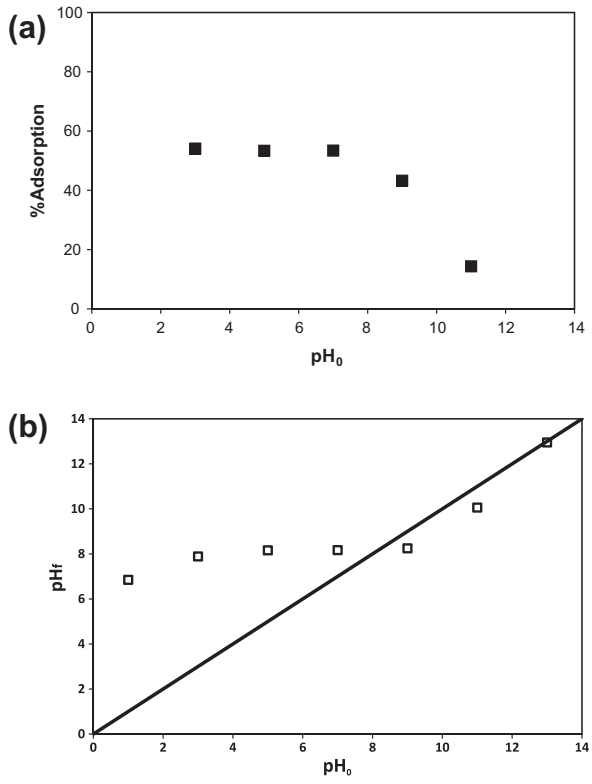

Fig. 2. Influence of pH. (a) Effect of pH on boron removal using [chiNi(II)]. (b) Variation in pH. $[B]_0$ = 50 mg L^{-1}, m = 1 g, V = 0.1 L, t = 72 h.

pH < 9.2

(18)

pH ⩾ 9.2

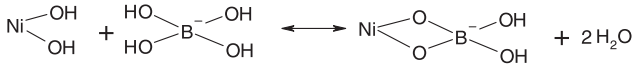

(19)

At pH < 9.25, boric acid is the predominant boron species; in addition, a weak interaction between the boron species and the NH_2 groups of chitosan was previously reported by Gazi and Shahmohammadi [18]. The pH of zero charge (pHpzc) was determined by acid–base titration [19] (Fig. AM4): At pH < 6.57, the surface is positively charged, indicating a higher affinity for anions $[B(OH)_4^-]$; at pH > 6.57, the surface becomes negatively charged and adsorption becomes favourable for the removal of H_3BO_3 species. As shown in Fig. 2a and b, a good adsorption occurs between pH 6.5 and 9.2, the predominant species (H_3BO_3) are attracted to the surface charged negatively.

3.3. Equilibrium studies

Sorption isotherms describe the distribution of the sorbate between the liquid and the solid phases at equilibrium. Fig. 3 compares the sorption isotherms at different pHs: the curves are characterised by the appearance of a saturation plateau at high boron concentration. The initial slopes are not very steep, indicating that the affinity of the sorbent for boron is not very strong. Langmuir and Freundlich models were tested: the Langmuir equation fitted the experimental data better than the Freundlich equation (Table 1). The maximum sorption capacity reached

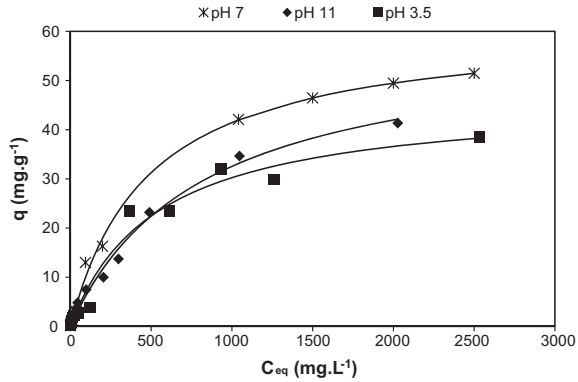

Fig. 3. Isotherm plots of boron adsorption using [chiNi(II)] composites. m = 0.04 g, V = 0.1 L, t = 72 h.

61.4 mg g^{-1}; the molar ratio between boron and $Ni(OH)_2$ was determined as the ratio between the maximum amount of sorbed boron (mmol) and the mass of $Ni(OH)_2$ (mmol) present in the adsorbent beads used to plot the isotherms. This value corresponds to 0.73 $mmol_B$ $(mmol_{Ni(OH)2})^{-1}$.

Parameter R_L (Eq. (20)), defined as a dimensionless separation factor, was used by Kavak [39] to determine if an isotherm is favourable or unfavourable:

$$R_L = \frac{1}{1 + bC_o} \tag{20}$$

where b is the Langmuir constant (L mg^{-1}). According to Öztürk and Kavak [5], the value of R_L characterises the shape of the isotherm:

R_L = 1 Linear
R_L > 1 Unfavourable
0 < R_L < 1 Favourable
R_L = 0 Irreversible

The R_L calculated with Eq. (20) indicated that boron adsorption with [chiNi(II)] is favourable at 20 °C, and for a concentration of boron of 50 mg L^{-1} (Table 1).

Table 2 shows a comparison of the maximum sorption capacities of materials found in the literature; the best operating conditions are also presented. [chiNi(II)] composites have a sorption capacity of the same order of magnitude as other sorbents; although calcined magnesite tailing [41] and NanoFe [42] present better q, [chiNi(II)] has an important advantage because it can be easily regenerated (see the following sections).

3.4. Influence of contact time

Fig. 4 shows the kinetic profile for the adsorption of boron using air-dried beads, freeze-dried beads and wet beads; all of the plots have a similar trend. Two steps can be observed: an initial fast sorption followed by a slow-rate step when approaching the equilibrium. The drying of beads influences both the adsorption capacity at equilibrium and the kinetic profile. In terms of the equilibrium sorption capacity, wet beads and air-dried beads have comparable values while the freeze-dried beads exhibit a much higher residual concentration. This surprising result can be explained by the poor mechanical stability of the freeze-dried material. Under blade-agitation, the freeze-dried beads tended to break and release the nickel (II) hydroxide sorbent into the solution. This may contribute to increase the amount of boron present in the solution. However, for wet and air-dried beads, the residual concentration was hardly affected: the most significant difference be-

Table 1
Langmuir and Freundlich constants of adsorbents.

pH_i	pH_f	Langmuir model				Freundlich model		
		q_{max} (mg g^{-1})	$b{\cdot}10^3$ (L mg^{-1})	r^2	r_{L50ppm}	k_F ($mg^{1-1/n}$ g^{-1} $L^{1/n}$)	n	r^2
3.5	7.4	46.30	1.88	0.97	0.91	1.00	2.09	0.92
7.1	7.9	61.41	2.07	0.98	0.90	0.58	1.61	0.98
11.0	11.0	59.12	1.22	0.98	0.94	0.69	1.83	0.95

Table 2
Comparison of boron sorption capacities for several adsorbents.

Adsorbent	T(K)	pH	q (mmol g^{-1})	Ce (mmol L^{-1})	Authors
Calcined magnesite tailing	318	6.0	6.1	50.9	Kipçak and Özdemir [41]
NanoFe	298	8.3	6.01	2.78E−02	Zelmanov and Semiat [42]
[chiNi(II)]	298	7	5.68	231.3	This work
Fe-impregnated GAC	298	8.3	4.63	2.78E−02	Zelmanov and Semiat [42]
CTS-MG	298	7.0	3.25	17.0	Wei et al. [19]
Polymer supported iminodipropylene glycol functions	298	6.0–6.5	3.0	430.0[a]	Senkal and Bicak [43]
ATG	303	8.8	2.25	14.1	Morisada et al. [44]
GlyPSF	303	7	2.09	87.9	Meng et al. [45]
Polymer supported 2-hydroxylethylamino glycol functions	298	7.4	1.82	485.0[a]	Gazi and Bicak [46]
Si-MG	298	7.0	1.54	0.2	Xu et al. [47]
TG	303	8.8	1.05	14.3	Morisada et al. [44]
Amberlite IRA-743	298	7.0	0.71	8.0	Wei et al. [19]
Fly ash	318	10.0	0.64	7.7	Polowczyk et al. [48]
CCTS	298	7.0	0.39	8.0	Wei et al. [19]
Calcined Alunite	298	10.0	0.31	16.7	Kavak [40]
Al-WTRs	298	8.3	9.07E-02	7.4	Irawan et al. [49]
Palm oil mill boiler bottom ash	298	8.0	4.35E-02	1.2	Chong et al. [50]

[a] Initial boron concentrations (mmol L^{-1}).

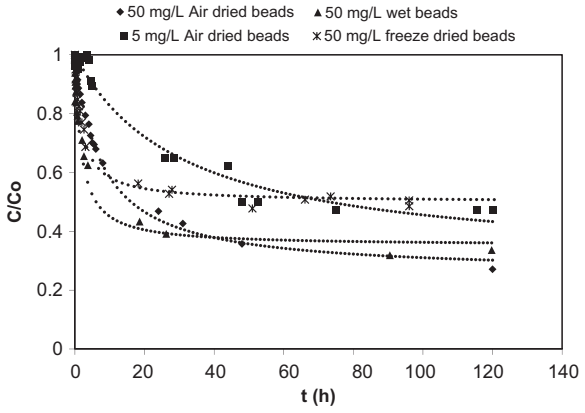

Fig. 4. Effect of contact time on [chiNi(II)] composites. pH = 11, m = 1.1 g, V = 0.5 L, t = 120 h.

tween the two materials was observed at the time required to reach equilibrium (approximately 17 h for wet beads versus 48 h for air-dried beads). The active sites in the wet beads are more easily accessible to the adsorbate molecules, and consequently the time to reach equilibrium is lower. The differences between the three materials can also be detected in the initial section of the curves: while for wet and freeze-dried beads the curves were almost overlapped, in the case of air-dried beads the initial slope of the kinetic profile was lower. This is probably because the air-dried beads are smaller in size (0.85 mm vs. 2 mm) with a direct impact on the interfacial surface area and that the re-hydration of the sorbent particles takes a longer time (which, in turn, affects the diffusion properties and mass transfer).

In addition, decreasing the concentration of boron significantly decreased the sorption kinetics both in the initial section (usually governed by the resistance to film diffusion) and in the final section (affected by the resistance to intraparticle diffusion). Decreasing the boron concentration decreased the concentration gradient between the solution and the surface of the sorbent, and between the surface of the solution and the core of the sorbent. As a consequence, the driving force decreased as well as the sorption rate.

Table 3 reports the comparison of the experimental sorption capacities at equilibrium with calculated values for both the pseudo-first order and the pseudo-second order rate equation models (PFORE and PSORE). The comparison of the correlation coefficients confirms that the pseudo-second order model is the most appropriate for fitting the experimental data.

The simplified equation for evaluating the contribution of the resistance to intraparticle diffusion (Eq. (7)) was tested (see Fig. AM5 in Additional Material Section). The linear plot did not

Table 3
Pseudo-first-order and pseudo-second-order kinetic parameters for the removal of boron from aqueous solutions.

Adsorbent	Pseudo-first order model					Pseudo-second order model				
	$[B]_0$ mg L^{-1}	q_{exp} mg g^{-1}	K_1 min^{-1}	q_1 mg g^{-1}	r^2	K_2 min^{-1}	q_2 mg g^{-1}	r^2	Kp mg g^{-1} $min^{-1/2}$	D_e cm^2 s^{-1}
Air dried beads (Ø 0.85 mm)	50	7.56	1.99×10^{-3}	6.60	0.98	2.75×10^{-4}	7.71	0.99	0.20	3.0×10^{-9}
Air dried beads (Ø 0.85 mm)	5	0.55	5.80×10^{-4}	0.57	0.97	7.12×10^{-4}	0.74	0.97	0.02	2.3×10^{-9}
Wet beads (Ø 2 mm)	50	6.35	6.34×10^{-3}	5.91	0.89	1.48×10^{-3}	6.21	0.93	0.23	6.8×10^{-8}
Freeze dried beads (Ø 2 mm)	50	4.48	6.11×10^{-3}	4.77	0.97	1.66×10^{-3}	4.98	0.98	0.22	1.6×10^{-8}

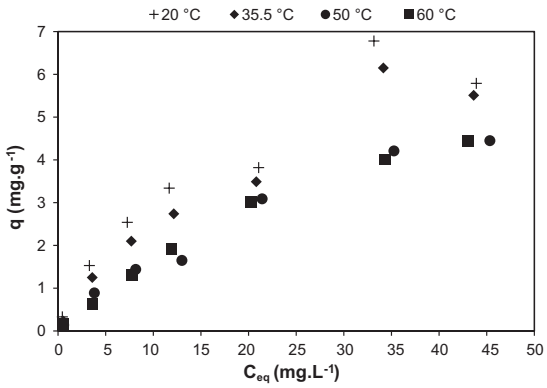

Fig. 5. Effect of temperature on boron adsorption pH = 7, m = 0.04 g, V = 0.1 L, t = 72 h.

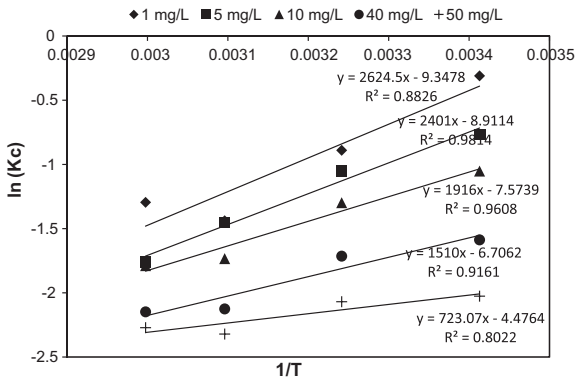

Fig. 6. Van't Hoff plot of boron adsorption on [chiNi(II)] composites. pH = 7, m = 0.04 g, V = 0.1 L, t = 72 h.

pass through the origin, indicating that intraparticle diffusion is not the unique step that controls the boron uptake kinetics. The resistance to film diffusion may affect the control of uptake kinetics. *Kp* values (Table 3) were obtained from the slope of the linear portions of the kinetics profiles. Results generally show that increasing the boron concentration and the particle size increased the intraparticle diffusion rate constant.

Diffusion coefficients (D_e) were calculated using the Crank equation for the different kinetics profiles. Table 3 shows that the intraparticle diffusion coefficient decreased according to the series: Wet beads > freeze-dried beads > air-dried beads. The differences between the diffusion coefficients of freeze-dried beads and air-dried beads may be attributed to several causes: (i) difficulty of access to active sites (OH^- and NH_2 groups) in the adsorbent after drying, (ii) fragility of the organic matrix after freeze drying, and (iii) a dual (resistance to film and intraparticle diffusion), rather than a single diffusion mechanism [21].

Another cause (not very evident in this study) suggested by Rorrer et al. [51], may be used to explain this trend: (iv) a pore blockage mechanism, where at low concentrations, the sorbed species flux is low at the entrance of the porous network, resulting in the accumulation of the adsorbate species at the opening of the polymer network and a final blockage of the pore entrance. The diffusion coefficient (with air dried beads) with boron solutions containing concentrations of 5 mg L^{-1} and 50 mg L^{-1} reached 2.3×10^{-9} and 3.0×10^{-9} cm^2 s^{-1}, respectively. The values obtained are comparable with the values obtained in the literature [52]. Vasudevan et al. [52] and Yang and Al-Duri [53] have reported that the diffusivity coefficient for chemisorption systems should have a magnitude of 10^{-5} to 10^{-13} cm^2 s^{-1}.

Table 4
Thermodynamic parameters.

$[B]_o$ (mg L^{-1})	Temperature (K)	*Kc*	ΔG° $\left(\frac{kJ}{mol}\right)$	ΔH° $\left(\frac{kJ}{mol}\right)$	ΔS° $\left(\frac{kJ}{mol}\right) \times 10^{-2}$
1	293.0	0.73	0.75	−21.82	−7.84
	308.5	0.41	2.28		
	323.0	0.23	3.86		
	333.6	0.27	3.59		
5	293.0	0.46	1.86	−19.96	−7.41
	308.5	0.34	2.70		
	323.0	0.23	3.90		
	333.6	0.17	4.88		
10	293.0	0.34	2.56	−15.92	−6.29
	308.5	0.27	3.32		
	323.0	0.17	4.65		
	333.6	0.16	4.95		
40	293.0	0.20	3.86	−12.55	−5.57
	308.5	0.18	4.39		
	323.0	0.12	5.70		
	333.6	0.11	5.95		
50	293.0	0.13	4.93	−6.01	−3.72
	308.5	0.12	5.30		
	323.0	0.09	6.23		
	333.6	0.10	6.29		

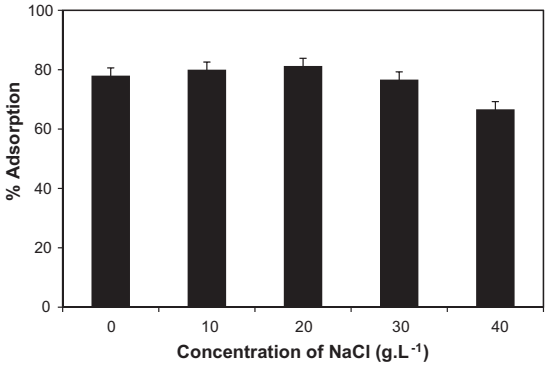

Fig. 7. Influence of NaCl on boron adsorption. $[B]_0$ = 5 mg L^{-1}, m = 0.22 g, pH = 7, V = 0.1 L, t = 72 h.

3.5. Effect of temperature

Fig. 5 shows the effect of the temperature (in the range of 20–60 °C) on boron adsorption; sorption capacity decreased when temperature increased, indicating that boron sorption by [chiNi(II)] is exothermic. According to the results reported in Table 4 and Fig. 6, the negative values of entropy and enthalpy changes correspond to a decrease in the degree of freedom of the adsorbed species, and the positive values of Gibbs energy (ΔG°) at 293 and 313 K indicate that adsorption is not spontaneous at these temperatures. This behaviour was also observed by Kavak [40], who investigated boron sorption at different temperatures using calcined alunite.

Kavak [39] reported that the enthalpy change between 0 and 20 kJ^{-1} mol^{-1} corresponds to a physisorption process, while in the case of chemisorption, the enthalpy change ranges between 80 kJ mol^{-1} and 400 kJ mol^{-1}. Boron removal from [chiNi(II)] composites proceeds through a chemical sorption in contradiction with the values presented in the literature [40].

3.6. Influence of NaCl on boron removal

To determine the influence of the ionic strength on the effectiveness of [chiNi(II)], sodium chloride was added to the boron

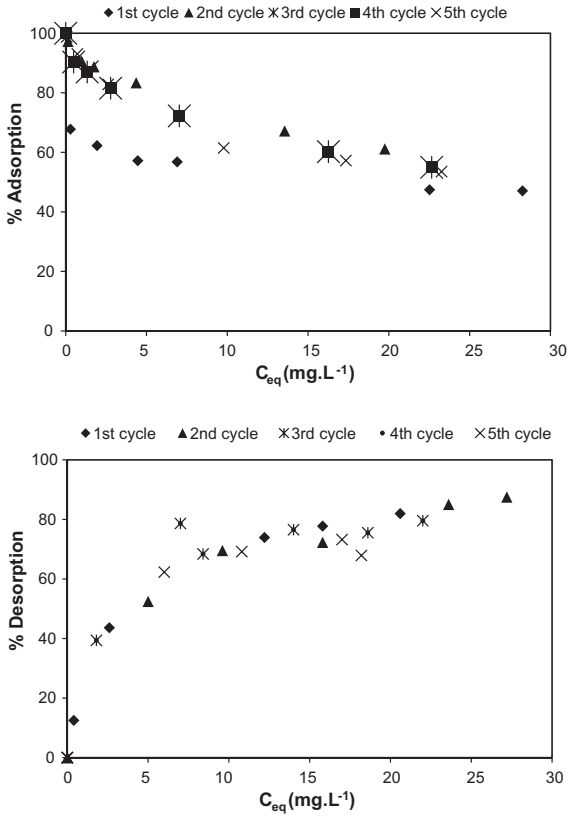

Fig. 8. Adsorption and desorption cycles in boron removal from aqueous solutions. m = 0.22 g, pH = 7, V = 0.1 L, t = 72 h.

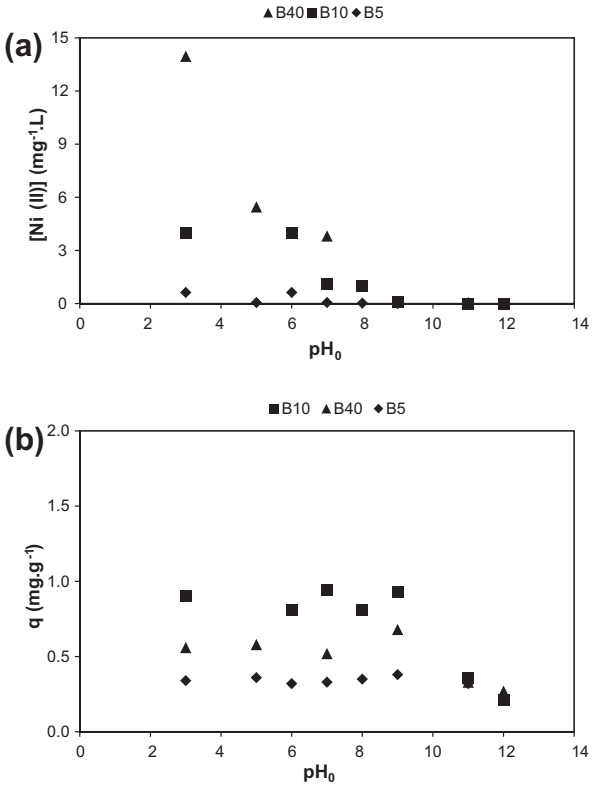

Fig. 9. Effect of pH using different beads. (a) Release of Ni (II) as a function of pH. (b) Influence of pH on the sorption capacity of adsorbents. $[B]_0$ = 5 mg L^{-1}, m = 0.1 g, V = 0.1 L, t = 72 h.

solution up to a concentration of 40 g L^{-1}. Fig. 7 shows that the boron removal efficiency remained constant until a 30 g L^{-1} NaCl concentration. When the NaCl concentration reached 40 g L^{-1}, a slight reduction (approximately 10%) was observed: the ionic strength has a weak influence on the boron sorption properties of the [chiNi(II)] composite. This makes it possible to use the adsorbent in seawater (reported to have an average salinity of approximately 35 g L^{-1}, [54]). Unrefined sea salt contains approximately 98% of sodium chloride (NaCl) (the remaining 2% consists of other salts made up of calcium, magnesium and potassium and the bromide and sulphate ions [54]). Preliminary studies with samples of sea water from the Mediterranean Sea (salinity 35 g L^{-1} and boron concentration 4.2 mg L^{-1}) showed that the adsorbent could be used to recover boron from sea water. No influence of salinity on boron adsorption capacity was detected.

3.7. Adsorption–desorption cycles

Several adsorption–desorption cycles were performed to verify the possibility to reuse the sorbent and to recover boron from aqueous solutions. Fig. 8 compares the sorption and desorption efficiencies for five successive cycles. While the sorption efficiency reached 70% in the first cycle, the removal efficiency increased up to 80–100% for the next cycles. This surprising trend is probably due to the negative effect of the presence of free nickel (not reacted with OH^- to form nickel (II) hydroxide) in the first step. After sorption/desorption and washing of the sorbent, the free nickel is released from the resin. As a consequence, the stabilised material increases its efficiency for boron removal for the next sorption steps.

Fig. 8 shows that water at pH 12 is an efficient eluent, and boron can be recovered from the loaded sorbent. This is a great advantage

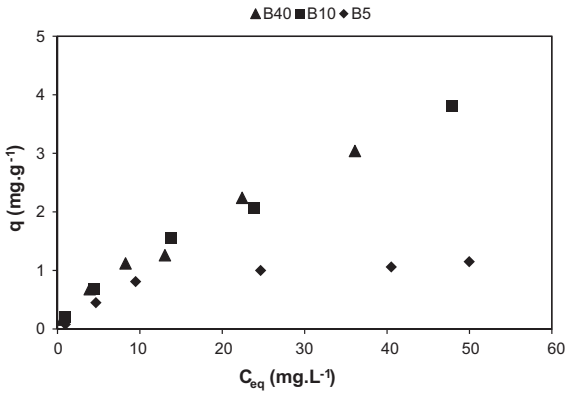

Fig. 10. Sorption isotherms using different beads. m = 0.1 g, pH = 7, V = 0.1 L, t = 72 h.

in comparison with other commercial sorbents such as ion exchange resins, which require more expensive eluents for sorbent regeneration [1] (for example, 0.5 M HCl for Dowex 2×8 resins [55] and 5% H_2SO_4 [56] for Diaion CRB 02 resins). The boron recovery from the loaded sorbent ranges between 70% and 90% for the five cycles.

3.8. Control of nickel ion release

The stability of the sorbent was investigated, analysing the release of Ni(II) (together with boron removal at different pHs, Fig. 9). When the pH reaches 9, nickel precipitates and can be collected by filtration. The World Health Organization recommends a guideline value of 0.07 mg L^{-1} [2] for the element nickel in drink-

ing water. It is important to note that this leakage of nickel from the beads is due to the large amount of nickel nitrate used for sorbent manufacturing: A part of this excess nickel did not fully react with NaOH, allowing this fraction to be readily released into the solution.

To verify this hypothesis, three different sorbents containing variable amounts of nickel (B40, B10 and B5) were prepared following the same procedure described in Section 2.2. Fig. 9a shows the release of nickel from the three types of beads. As expected, the amount of nickel released from the sorbent increases with Ni(II) content in the composite. B10 beads showed a significantly lower release of nickel, whereas B5 nickel release is very small in acidic solutions. At pH > 9 nickel ions were not detectable in solution.

The mass percentage of $Ni(OH)_2$ in B40, B10 and B5 composites was determined to be 72%, 45% and 18%, respectively. Therefore, the nickel release in solution at an acidic pH can be attributed to excess nickel that did not react with the NaOH solution during sorbent synthesis.

In Figs. 9b and 10, it is shown that an increase in the nickel concentration (in the beads) contributes to an increase in the sorption capacity, as was expected. However, Fig. 10 shows B10 and B40 have a similar sorption capacity. Two causes can explain this: (i) the release of nickel in B40 is much greater than in B10, hence the amount of nickel (II) hydroxide that remained in B40 is the same in magnitude as the $Ni(OH)_2$ present in B10. (ii) It is possible that a large amount of nickel was used in the preparation of the B40 beads (and did not react completely with NaOH solution), and so it remains free on the composite and can hinder access of boron molecules to the active sites of [chiNi(II)] (OH^- and NH_2 groups).

Therefore, the best beads used in this work for adsorption of boron (in terms of their stability and their sorption capacity) were the B10 beads.

4. Conclusions

[ChiNi(II)] is an efficient sorbent for the removal of boron. A temperature study confirmed the exothermic nature of boron sorption. TGA analysis revealed that the composite is thermally stable and that its decomposition starts at 531 K. The maximum sorption capacity of 61.4 mg g^{-1} was reached at 298 K and at a pH of 8–9. The Langmuir model fit the sorption isotherms well. At a pH of 9, good sorption and good stability of nickel on the sorbent simultaneously occurs. The Kinetic profiles were best fitted by the pseudo-second order rate equation (compared to the pseudo-first order model).

Desorption studies showed the high efficiency for boron recovery using water at a pH of 12. Five consecutive cycles were performed, and desorption uptake remained higher than 90% in almost all cycles. The presence of NaCl at concentration as high as 35 g L^{-1} does not significantly affect the boron removal from aqueous solutions.

Acknowledgements

This work was supported by the Ministry of Science and Innovation of Spain (Project No. CTQ 2011-22412). The authors would like to thank Mr. Jean Marie Taulemesse and Mr. André Brun for their assistance in this project.

References

[1] N. Ostürk, D. Kavak, T. Ennil, Boron removal from aqueous solution by reverse osmosis, Desalination 223 (2008) 1–9.
[2] World health organization, Guidelines for drinking-Water quality, fourth ed., Geneva, 2011.
[3] N. Hilal, G.J. Kim, C. Somerfield, Boron removal from saline water: a comprehensive review, Desalination 273 (2011) 23–35.
[4] S. Karahan, M. Yurdakoç, Y Seki, K. Yurdakoç, Removal of boron from aqueous solutions by clays and modified clays, J. Colloid Interf. Sci. 293 (2006) 36–42.
[5] N. Öztürk, D. Kavak, Adsorption of boron from aqueous solutions using fly ash: batch and column studies, J. Hazard. Mater. B127 (2005) 81–88.
[6] M. Simonnot, C. Castel, M. Nicolai, C. Rosin, M. Sardin, H. Jauffret, Boron removal from drinking water with a boron selective resin: is the treatment really selective?, Water Res 34 (2004) 109–116.
[7] N. Kabay, S. Sarp, M. Yuksel, M. Kitis, H. Koseoglub, Ö. Arar, M. Bryjak, R. Semiat, Removal of boron from SWRO permeate by boron selective ion exchange resins containing N-methylglucamine groups, Desalination 223 (2008) 49–56.
[8] D. Prats, M.F. Chillon-Arias, M. Rodriguez-Pastor, Analysis of the influence of pH and pressure on the elimination of boron in reverse osmosis, Desalination 128 (2000) 269–273.
[9] M. Rodríguez-Pastor, A. Ferrándiz-Ruiz, M.F. Chillon, D. Prast-Rico, Influence of pH in the elimination of boron by means of reverse osmosis, Desalination 140 (2001) 145–152.
[10] Y. Cengeloglu, G. Arslan, A. Tor, I. Kocak, N. Dursun, Removal of boron from water by using reverse osmosis, Sep. Purif. Technol. 64 (2008) 141–146.
[11] Z. Yazicigil, Y. Oztekin, Boron removal by electrodialysis with anion-exchange membranes, Desalination 190 (2006) 71–78.
[12] T. Itakura, R. Sasai, H. Itoh, Precipitation recovery of boron from wastewater by hydrothermal mineralization, Water Res. 39 (2005) 2543–2548.
[13] A. Erdem, A. Yilmaz, R. Boncukcuoğlu, M. Muhtar-Kocakerim, A quantitative comparison between electrocoagulation and chemical coagulation for boron removal from boron-containing solution, J. Hazard. Mater. 149 (2007) 475–481.
[14] A.S. Koparal, The removal of salinity from produced formation by conventional and electrochemical methods, Fresen. Environ. Bull. 12A (2002) 1071–1077.
[15] H. Demey, M. Ruiz, J.A. Barron-Zambrano, A.M. Sastre, Boron removal from aqueous solutions using alginate gel beads in fixed bed systems, J. Chem. Technol. Biot. (in press) (JCTB-13-0429.R1).
[16] M. Ruiz, C. Tobalina, H. Demey-Cedeño, J.A. Barron-Zambrano, A.M. Sastre, Sorption of boron on calcium alginate gel beads, React. Funct. Polym. 73 (2013) 635–657.
[17] M. Ruiz, L. Roset, H. Demey, S. Castro, A.M. Sastre, J.J. Pérez, Equilibrium and dynamic studies for adsorption of boron on calcium alginate gel beads using principal component analysis (PCA) and partial least squares (PLS), Mat.-wiss. U. Werkstofftech. 44 (2013) 410–415.
[18] M. Gazi, S. Shahmohammadi, Removal of trace boron from aqueous solution using iminobis-(propylene glycol) modified chitosan beads, React. Funct. Polym. 72 (2012) 680–686.
[19] Y.T. Wei, Y.M. Zheng, J.P. Chen, Design and fabrication of an innovative and environmental friendly adsorbent for boron removal, Water Res. 45 (2011) 2297–2305.
[20] M. Turek, P. Dydo, J. Trojanowska, A. Campen, Adsorption/Co-precipitation – reverse osmosis system for boron removal, Desalination 205 (2007) 192–199.
[21] M. Ruiz, A.M. Sastre, M.C. Zikan, E. Guibal, Palladium sorption on glutaraldehyde-crosslinked chitosan in fixed-bed systems, J. Appl. Polym. Sci. 81 (2001) 153–165.
[22] E. Guibal, A. Larkin, T. Vincent, J.M. Tobin, Chitosan sorbents for platinum sorption from dilute solutions, Ind. Eng. Chem. Res. 38 (1999) 401–412.
[23] C. Vincent, A. Hertz, T. Vincent, Y. Barré, E. Guibal, Immobilization of inorganic ion-exchange into biopolymer foams-Application to cesium sorption, Chem. Eng. J. 236 (2014) 202–211.
[24] I. Langmuir, The adsorption of gases on plane surfaces of glass, mica and platinum, J. Am. Chem. Soc. 40 (1918) 1361–1403.
[25] H.M.F. Freundlich, Über die adsorption in lösungen, Z. Phys. Chem. 57A (1906) 385–470.
[26] C. Nemasivayam, R.T. Yamuna, Adsorption of direct red 12B by biogas residual slurry: equilibrium and rate processes, Environ. Pollut. 89 (1995) 1–7.
[27] S. Lagergreen, Zur theorie der sogenannten adsorption gelöster stoffe: kungliga Svenska Vetenskapsakademiens, Handlingar 24 (1898) 1–39.
[28] Y.S. Ho, G. McKay, Sorption of dye from aqueous solution by peat, Chem. Eng. J. 70 (1998) 115–124.
[29] J. Crank, The Mathematics of Diffusion, second ed., Oxford University Press, Oxford, 1975.
[30] P. Vishnu-Kamath, G.N. Subbanna, Electroless nickel hydroxide: synthesis and characterization, J. Appl. Electrochem. 22 (1992) 478–482.
[31] G.Z. Kyzas, M. Kestoglou, N.K. Lazaridis, D.N. Bikiaris, N-(2-Carboxybenzyl) grafted chitosan as adsorptive agent for simultaneous removal of positively and negatively charged toxic metal ions, J. Hazard. Mater. 244–245 (2013) 29–38.
[32] E.A. Bursali, Y. Seki, S. Seyhan, M. Delener, M. Yurdakoç, Synthesis of chitosan beads as boron sorbents, J. Appl. Polym. Sci. 122 (2011) 657–665.

[33] T.N. Ramesh, P. Vishnu-Kamath, Synthesis of nickel hydroxide: effect of precipitation conditions on phase selectivity and structural disorder, J. Power Sources 156 (2006) 655–661.
[34] A.N. Ay, B.N. Karan, A. Temel, Boron removal by hydratalcite-like, carbonate-free Mg–Al–NO3–LDH and a rationale on the mechanism, Micropor. Mesopor. Mat. 98 (2007) 1–5.
[35] A. Olgun, N. Atar, Equilibrium, thermodynamic and kinetic studies for the adsorption of lead (II) and nickel (II) onto clay mixture containing boron impurity, J. Ind. Eng. Chem. 18 (2012) 1751–1757.
[36] P. Sorlier, C. Viton, A. Domard, Relation between solution properties and degree of acetylation of chitosan: role of aging, Biomacromolecules 3 (2002) 1336–1342.
[37] M. Pagznl, D. Lemarchand, A. Spivack, J. Gaillardet, A critical evaluation of the boron isotope pH proxy: the accuracy of ancient ocean pH estimates, Geochim. Cosmochim. Ac. 69 (4) (2005) 953–961.
[38] D. Schubert, Borates in industrial use, Struct. Bond. 105 (2003) 1–40.
[39] V. Lubes, L. Véliz, J.D. Martinez, M.L. Araujo, F. Brito, G. Lubes, M. Rodriguez, Estudio de la hidrólisis del ion Niquel (II) y de la formación de los complejos de Niquel (II) con los acidos Picolinico y Dipicolinico en NaCl 1,0 mol dm^{-3} a 25 °C, Avances en Química 6 (1) (2011) 3–8.
[40] D. Kavak, Removal of boron from aqueous solutions by batch adsorption on calcined alunite using experimental design, J. Hazard. Mater. 163 (2009) 308–314.
[41] I. Kipçak, M. Özdemir, Removal of boron from aqueous solution using calcined magnesite tailing, Chem. Eng. J. 189–190 (2012) 68–74.
[42] G. Zelmanov, R. Semiat, Boron removal from water and its recovery using iron (Fe^{+3}) oxide/hydroxide-based nanoparticles (NanoFe) and NanoFe-impregnated granular activated carbon as adsorbent, Desalination 333 (2014) 107–117.
[43] B.F. Senkal, N. Bicak, Polymer supported iminodipropylene glycol functions for removal of boron, React. Funct. Polym. 55 (2003) 27–33.
[44] S. Morisada, T. Ogata, Y.H. Kim, Y. Nakano, Adsorption removal of boron in aqueous solutions by amine-modified tannin gel, Water Res. 45 (2011) 4028–4034.
[45] J. Meng, J. Yuan, Y. Kang, Y. Zhang, Q. Du, Surface glycosylation of polysulfone membrane towards a novel complexing membrane for boron removal, J Colloid Interf. Sci. 368 (2012) 197–207.
[46] M. Gazi, N. Bicak, Selective boron extraction by polymer supported 2-hydroxylethylamino propylene glycol functions, React. Funct. Polym. 67 (2007) 936–942.
[47] L. Xu, Y. Liu, H. Hu, Z. Wu, Q. Chen, Synthesis, characterization and application of a novel silica based adsorbent for boron removal, Desalination 294 (2012) 1–7.
[48] I. Polowczyk, J. Ulatowska, T. Kozlecki, A. Bastrzyk, W. Sawikski, Studies on removal of boron from aqueous solution by fly ash agglomerates, Desalination 310 (2013) 93–101.
[49] C. Irawan, J.C. Liu, C.C. Wu, Removal of boron using aluminum-based water treatment residuals (Al-WTRs), Desalination 276 (2011) 322–327.
[50] M.F. Chong, K.P. Lee, H.J. Chieng, I.I. Ramli, Removal of boron from ceramic industry wastewater by adsorption-flocculation mechanism using palm oil mill boiler (POMB) bottom ash and polymer, Water Res. 43 (2009) 3326–3334.
[51] G.L. Rorrer, T.-Y. Hsien, J.D. Way, Synthesis of porous-magnetic chitosan beads for removal of cadmium ions from waste water, Ind. Eng. Chem. Res. 32 (1993) 2170–2178.
[52] S. Vasudevan, J. Lakshmi, G. Sozhan, Electrochemically assisted coagulation for the removal of boron from water using zinc anode, Desalination 310 (2013) 122–129.
[53] X.-Y. Yang, B. Al-Duri, Application of branched pore diffusion model in the adsorption of reactive dyes on activated carbon, Chem. Eng. J. 83 (2001) 15–23.
[54] N. Gros, M.F. Camoes, C. Oliveira, M.C.R. Silva, Ionic composition of seawaters and derived saline solutions determined by ion chromatography and its relation to other water quality parameters, J. Chromatogr. A 1210 (2008) 92–98.
[55] N. Öztürk, T. Ennil-Köse, Boron removal from aqueous solutions by ion-exchange resin: batch studies, Desalination 227 (2008) 233–240.
[56] N. Kabay, S. Sarper, M. Yuksel, Ö. Arar, M. Bryjak, Removal of boron from seawater by selective ion exchange resins, React. Funct. Polym. 67 (2007) 1643–1650.